Theor Chem Acc (2002) 108:150–156
DOI 10.1007/s00214-002-0370-x

Theoretical Chemistry Accounts

Regular article

Electron localization function for transition-metal compounds

Miroslav Kohout, Frank Richard Wagner, Yuri Grin

Max-Planck-Institut für Chemische Physik fester Stoffe, Nöthnitzer Strasse 40, 01187 Dresden, Germany

Received: 20 February 2002 /Accepted: 14 June 2002 /Published online: 19 August 2002

Abstract. The analysis of the electron localization function of molecules and solids needs to involve the atomic core regions as well to reveal a more detailed insight into the bonding situation.

Key words: Electron localization function – Bonding – *d* orbitals

1 Introduction

The electron localization function (ELF) is widely used to describe and visualize chemical bonds in molecules and solids [1]. The ELF in the formulation of Becke and Edgecombe is based on the ratio $\chi_{BE}(\mathbf{r}) = D(\mathbf{r})/D_h(\mathbf{r})$, where $D(\mathbf{r})$ is the curvature of the spherically averaged probability density to find close to a reference electron (located at the position **r**) another same-spin electron and $D_h(\mathbf{r})$ is the corresponding expression for a uniform electron gas of the same electron density [2]. The essential quantity for the derivation of the ELF formula of Becke and Edgecombe is the Hartree–Fock same-spin pair density. On the other hand, according to Savin et al. [3] the ELF can be seen as the ratio $\chi_S(\mathbf{r}) = t_P(\mathbf{r})/t_h(\mathbf{r})$ of the Pauli kinetic energy density, $t_P(\mathbf{r})$, at the position **r** and the kinetic energy density, $t_h(\mathbf{r})$, of a uniform electron gas of the same electron density. In this case the pair density is not needed for the derivation of the ELF formula. In both formulations, the ELF compares a measure of the local Pauli repulsion in the system examined with that in a uniform electron gas of the same density. Thus, the ELF cannot reveal any information about the actual magnitude of the Pauli repulsion. In the Hartree–Fock approximation $\chi_{BE}(\mathbf{r}) = \chi_S(\mathbf{r}) = \chi(\mathbf{r})$ (separately for each spin). Becke and Edgecombe introduced for the ELF the scaling $\eta(\mathbf{r}) = 1/[1 + \chi(\mathbf{r})^2]$, which bounds the ELF values between 0 and 1.

Although often claimed in the literature, low ELF values cannot be attributed to high Pauli repulsion. In the sense of Becke and Edgecombe or of Savin et al., ELF values below 0.5 only mean that the Pauli repulsion in the region analyzed is higher than in a uniform electron gas of the same density. It can easily be seen that it is not possible to deduce from the ELF value $\eta(\mathbf{r})$ at the position **r** the actual value of the Pauli repulsion, i.e. the value of the Pauli kinetic energy density $t_P(\mathbf{r})$ or the curvature of the spherically averaged probability density $D(\mathbf{r})$, respectively, because the ratio $\chi(\mathbf{r})$ depends on the electron density, which determines the respective $D_h(\mathbf{r})$ and $t_h(\mathbf{r})$ at this position, as well. The ELF does not mirror the Pauli repulsion [4]! Sometimes it can be found in the literature that low ELF values are characteristic for regions of low electron density [5, 6]. This is obviously not correct. Recall that in case of alkali-metal atoms the ELF and the electron density reach asymptotically 1 and 0 in outer regions, respectively [2]. Moreover, the ELF shows minima near the nucleus where the electron density can reach very high values.

Also, $\eta(\mathbf{r}) = 0.5$ indicates only that the Pauli repulsion at that position has the same value as in a uniform electron gas of the same density. Nevertheless, the system cannot be equated with the uniform electron gas (the density gradient in atoms and molecules is almost everywhere very different from zero) classifying it at the position examined as ''perfectly delocalized'' [5, 7] (in this case we encounter a dilemma to classify electrons in regions of $\eta(\mathbf{r}) < 0.5$).

ELF values close to 1 correspond to a situation where the local Pauli repulsion is very small compared to that in a uniform electron gas. Nevertheless, the local Pauli repulsion itself need not be small (bear in mind that close to the nucleus the ELF attains high values, but so does the Pauli repulsion).

2 Theory

As the goal of this work is connected with the capability of the ELF to exhibit the shell structure of atoms [2, 8] in a quantitative manner, we start by giving a short summary on this property.

Dedicated to Prof. Ole Krogh Andersen on the occasion of his 60th birthday

Correspondence to: M. Kohout
e-mail: kohout@cpfs.mpg.de

The term "atomic shell" is actually used for two different, but related representations. An atomic shell in the orbital picture is given by orbitals with the same principal quantum number, therefore spreading over the whole real space. The charge densities of the atomic shells interpenetrate. In contrast, the ELF for an atom reveals a radial sequence of ELF attractors around the nucleus [2, 8]. Between two successive attractors a repellor [9] is situated, which is used as the separatrix between two shell regions. Each shell region is thus separated from the neighboring shell regions by surfaces of zero flux in the ELF gradient and constitutes an ELF basin (in analogy to Bader's definition using the electron density and its gradient [10]). An "atomic shell" defined this way in the direct space as an atomic shell basin is strictly confined to a unique spacial region. The ELF has been shown to exhibit the shell structure of atoms not only in a qualitative manner, i.e. the number of atomic shell basins equals the number of atomic shells following from the Aufbau principle, but also in a quantitative manner: the electron density integrated within each atomic shell basin yields shell populations very close to those expected from the Aufbau principle [8]. From the orbital point of view, the charge found in a particular atomic shell basin originates mainly from orbitals with the same principal quantum number. The additional charge coming from orbitals with other principal numbers yields the observed "correct" electron population of the atomic shell basin.

For chemical aggregates of atoms, for example, molecules, the spherical symmetry is broken.[1] The atomic shell basin decomposes into several smaller basins interconnected by separatrices obeying the condition of zero flux in the ELF gradient, i.e. the zero-flux surfaces. Among the all points of the separatrices of two or more ELF basins at least one point exists which has the highest ELF value. This saddle point – besides attractor and repellor another critical point with zero ELF gradient – constitutes a basin interconnection point. We define a basin set as the join of sets of interconnected basins including a specified basin, where the basin interconnection points are above or equal to a given value (interconnection value).[2] With this definition we can now state the following observation. Usually each inner atomic shell basin decomposes into a number of basins which together form the shell basin set. A sufficient condition for this finding is that the highest intershell basin interconnection points obviously have lower ELF values than the lowest intrashell ones.

The common outermost basin set regions of all atoms constitute the valence region of the chemical system. The analysis of the topology of the ELF in this region has been proven to be an excellent tool to discuss various types of chemical bonding situations [1, 11]. However, the origin of the effects used to discuss chemical bonding in transition-metal compounds, where the *d* orbitals play an important role, has not yet been investigated in depth.

For completeness, we briefly mention two terms. The synaptic order of a valence basin – a widely used term in the topological analysis of the ELF – gives the number of core basins which have a common separatrix with the valence basin analyzed [12]. Synaptic order leaves out of account the ELF values at the basin interconnection points. An f-localization domain, another important term for the topological analysis of the ELF, is a region of space bounded by the isosurface $\eta(\mathbf{r}) = f$ [11]. For a basin set with the interconnection value $\eta_{ic} = f$ the f-localization domain is completely contained within the basin set. The number of members of the basin set equals the number of irreducible localization domains contained in the reducible f-localization domain.

3 Computational details

The calculations of atoms and the dimers were performed with the density functional program ADF [13]. The all-electron basis set IV (triple-zeta quality) was used. The bond distances of the dimers were optimized using a non-relativistic generalized gradient approximation all-electron calculation with the local density approximation (LDA) parameterization of Vosko, Wilk and Nusiar [14], the gradient correction of Becke [15] and the correlation correction of Lee, Yang and Parr [16]. We adhered to the one determinant level of theory to retain easy access to the traditional molecular orbital picture (of course, it is possible to use more elaborate methods, because the ELF is based on pair density or electron density, respectively). The ELF was calculated from the ADF results using the program DGrid [17]. For solid-state compounds, scalar relativistic all-electron LDA calculations were performed with the LMTO-ASA program with an ELF module already implemented [18]. The ELF distribution was analyzed with the Basin [19] and TopAn [20] program packages.

4 Results and discussion

According to the Aufbau principle (that means in the energy space), the penultimate atomic shell of a first-row transition metal is written as $3s^2 3p^6 3d^n$, followed by the valence shell $4s^1$ or $4s^2$. All the orbitals mentioned spread over the whole space. In contrast, in an ELF representation (that means in the real space), the outer-core shell basin is clearly separated from the other shell basins, taking up a well-defined region around the nucleus. The ELF diagram for scandium atom, the first member of the $3d$ transition metals and the ELF for germanium, an atom from the same row but with a filled

[1] In fact, all the spherical attractors and repellors of the ELF for an isolated atom are degenerate critical points, which means that this situation is topologically unstable and the very slightest perturbation is sufficient to break the spherical symmetry

[2] Using Fig. 1b (omitting the ELF distribution in the y direction) the definition of a basin set can be demonstrated. By choosing the interconnection value $\eta_{ic} = \eta(\mathbf{r}_1)$ the four outer core basins are joined into an outer core basin set. Taking the interconnection value $\eta_{ic} = \eta(\mathbf{r}_2)$, whereby $\eta(\mathbf{r}_2) < \eta(\mathbf{r}_1)$ leaves the outer core basin set unchanged, but additionally the four valence basins form a separate valence basin set. Finally, in case of the interconnection value $\eta_{ic} = \eta(\mathbf{r}_3)$, with $\eta(\mathbf{r}_3) < \eta(\mathbf{r}_2)$ the outer core and the valence basin sets unify into one single basin set

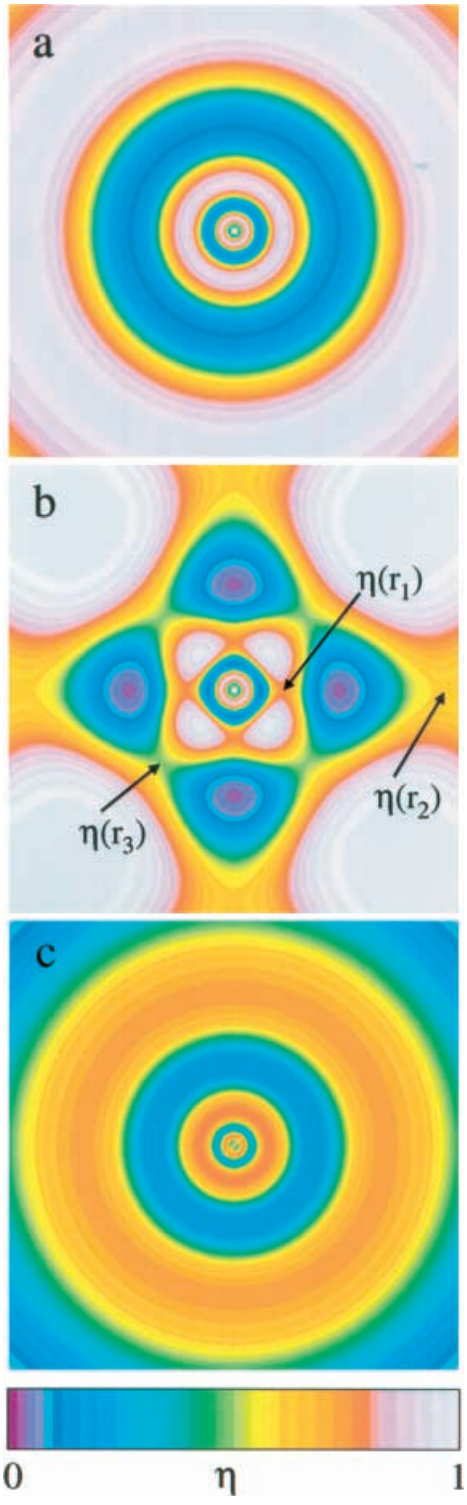

Fig. 1a–c. Electron localization function (ELF) for the atoms Sc and Ge. **a** Sc atom: all 3*d* orbitals are equally occupied. **b** Sc atom: only the $3d_{xz}$ orbital is occupied, both the outer-core and valence regions reveal pronounced structuring. Three ELF saddle points are marked. **c** Ge atom: fully occupied 3*d* orbitals. The ELF scale used in all the diagrams is at the bottom

3*d* shell are shown in Fig. 1. The value of the ELF maximum in the outer-core shell basin decreases with the increasing (evenly distributed) occupation of the *d* orbitals [4], see Fig. 1a for Sc ($3d_{xy}^{0.2}$ $3d_{xz}^{0.2}$ $3d_{yz}^{0.2}$ $3d_{x^2-y^2}^{0.2}$ $3d_{z^2}^{0.2}$) and Fig. 1c for Ge ($3d^{10}$). If the spherical symmetry is broken owing to the occupation of particular *d* orbitals, the ELF still achieves high values in some parts of the outer-core region, depending on the *d* orbitals occupied. The ELF diagram for the scandium atom in the case that only the $3d_{xz}$ orbital is occupied is shown in Fig. 1b. The influence of the $3d_{xz}$ orbital is clearly recognized in both the outer core and the valence region. An integration of the electron density in the penultimate-shell basin yields approximately $2+6+n$ electrons. The next (valence) shell basin contains about one or two electrons.

In the ELF diagram of a compound, the core region of each respective atom is spatially separated from the common valence region. The ELF for the Ge_2 molecule (triplet state with the $\sigma_g^2\sigma_u^2\pi_u^2\sigma_g^2$ configuration; bond distance 246 pm) is shown in Fig. 2. The spatial organization of the bonding between the germanium atoms can easily be recognized by the arrangement of the monosynaptic and disynaptic basins.

For bonds formed only by the outer-shell electrons, the ELF gives a description of the bonding situation that fits traditional ideas. If the penultimate-shell electrons participate in the bonding, for example, in $Li_6Ca_2[Mn_2N_6]$ with nonbridged Mn–Mn bonds of Mn(+4) [21]), then the description of the bonding requires a more detailed analysis of the ELF distribution. The question to answer is: what influence does the interaction of the inner-shell electrons have on the topology as well as on the electron numbers in the core and valence regions defined by the ELF [22]?

In case of the Sc_2 molecule (singlet state with the $\sigma_g^2\pi_u^4$ configuration; bond distance 221 pm) three ring-shaped localization domains with high ELF values, each en-

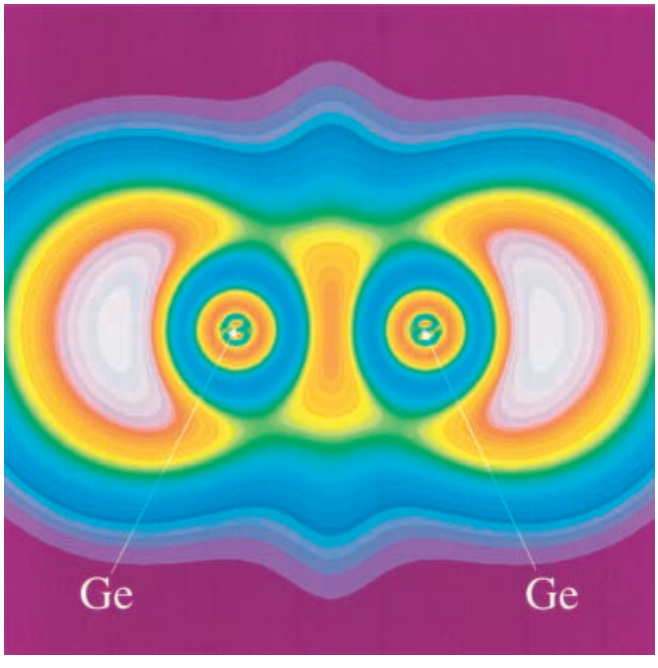

Fig. 2. Core regions and the common valence region for the Ge_2 molecule

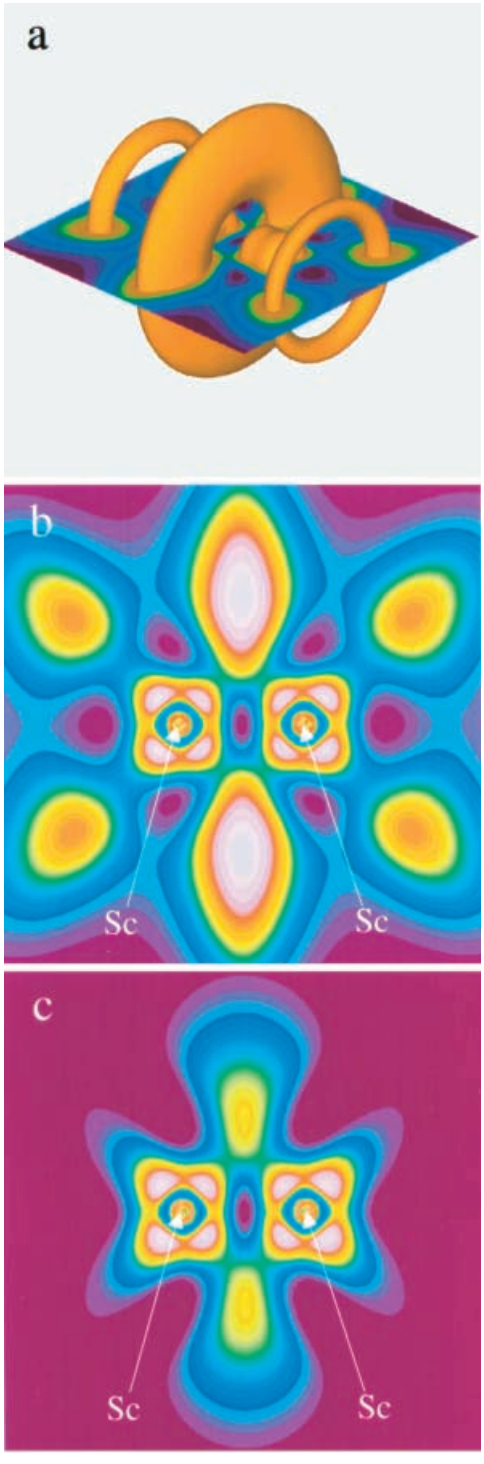

Fig. 3. **a** Rotationally symmetric 0.7-localization domain for the Sc_2 molecule. ELF slices through the Sc atoms for **b** Sc_2 molecule and **c** Sc_2^{2+} molecule

closing a ring attractor, are observed (Fig. 3a). One is located between the atoms; two others are positioned on the outer side of the molecule. Together they represent the bonding situation in direct space. There is no separation between a σ and a π bond in the ELF representation. In a simplified orbital picture of the Sc_2 molecule, the σ bond is represented by a linear combination of the 4*s* orbitals, whereas the π double bond (oriented along the *z*-axis) is given by a linear combination of the $3d_{xz}$ or $3d_{yz}$ orbitals. Therefore, the spherical symmetry of the outer-core shell basin is broken. Figure 3b shows clearly the structuring of the outer-core regions. The expected "π contribution" can be detected by the number of electrons in the ELF basin set of the multiple bond in the valence region. Thus, 3.4 electrons were found in the valence basin sets (0.4 electrons in the two monosynaptic basins and 2.6 electrons in the disynaptic one) of the Sc_2 molecule, i.e. 1.4 electrons more than expected for the σ bond. The same number of electrons is also obtained for Ti_2 ($\sigma_g^2\pi_u^4\sigma_g^2$ configuration) despite the quadruple bond shown by the orbital picture (the second σ bond is represented by a linear combination of the $3d_{z^2}$ orbitals).

For compounds where the inner-shell electrons participate in the homonuclear bonding, we find an excess of about 0.5 electrons per atom involved in the valence region. This feature still retained even if the valence-shell electrons do not participate in the bonding. Figure 3c shows the ELF diagram for the cation Sc_2^{2+} (singlet state with π_u^4 configuration; bond distance 217 pm). The ring in the valence region between the atoms is clearly separated from the core regions similarly to the neutral molecule Sc_2 and contains one electron despite the absence of occupied 4*s* orbitals in the molecular orbital scheme.

To clarify the results above we used a minimal basis set of Cartesian Slater functions $\psi_l = N_l x^i y^j z^k r^{n-l-1} \exp(-\alpha r)$; N_l, n and l are the normalization constant, the principal and the orbital quantum number, respectively to analyze whether the outer-core basin can be split in the ELF representation. The distance of the ELF maximum of an atomic shell from the nucleus is given by the exponent α of the Slater function $r_{max} = (n + 1/2)/\alpha$. For *s*, *p* and *d* orbital exponents of similar magnitude only one ELF maximum is obtained (the dashed line in Fig 4). If the *d* orbital exponent is pronouncedly smaller than the *s* and *p* exponents (that means a more diffuse

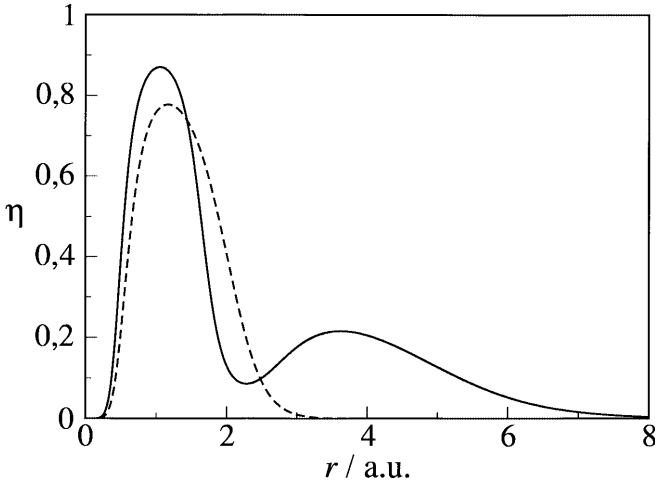

Fig. 4. ELF diagram simulating the outer-core region of the Sc atom using Cartesian Slater functions with different orbital exponents. *Dashed line*: 3*s*, 3*p*, and 3*d* exponents equal 3. *Solid line*: 3*s* and 3*p* exponents equal 3, whereas the 3*d* exponent equals 1

function), two maxima are obtained (the solid line in Fig. 4). If such diffuse *d* orbitals are favored for bonding, regions of high ELF values can form outside the core region, thus manifesting the participation of inner-shell electrons in the bonding in direct space. In this case a part of the electron density of the formerly atomic core shell basin is found in the (ELF defined) molecular valence region; however, this is not connected with considerable charge redistribution. Instead, the separatrices which define the space partitioning into the ELF basins are moving.

The structuring of the respective outer-core and valence regions, owing to the interaction of the inner-shell electrons, can also be observed if only one of the bonding partners is a transition-metal atom. The ELF diagram for the ScGa molecule (Fig. 5, the triplet state with the $\sigma^2\sigma^2\pi^2$ configuration; bond distance 271 pm) shows on the Sc side topological features similar to the Sc_2 molecule.

In ionic compounds large cations also exhibit a significant structuring of the outer-core region, as found Joubert et al. [23] for lanthanide trihalides (a similar core structuring of the density Laplacian of heavier alkaline-earth difluorides and dihydrides was reported by Bytheway et al. [24]). Although there is only moderate participation of the lanthanide 5*d* orbitals in the bonding, the decrease in the ELF values between the respective lanthanide and halogenide atoms cannot be attributed only to the increase of the Pauli repulsion between the ions. As mentioned already in the Introduction, the ELF does not mirror the Pauli repulsion.

The structuring of the core regions offers the opportunity to interpret the bonding situation in more complicated molecules as well. In the orbital picture, the single bond between the Re atoms in $Re_2(CO)_{10}$ is based mainly on the $5d_{z^2}$ orbitals of the metal atoms

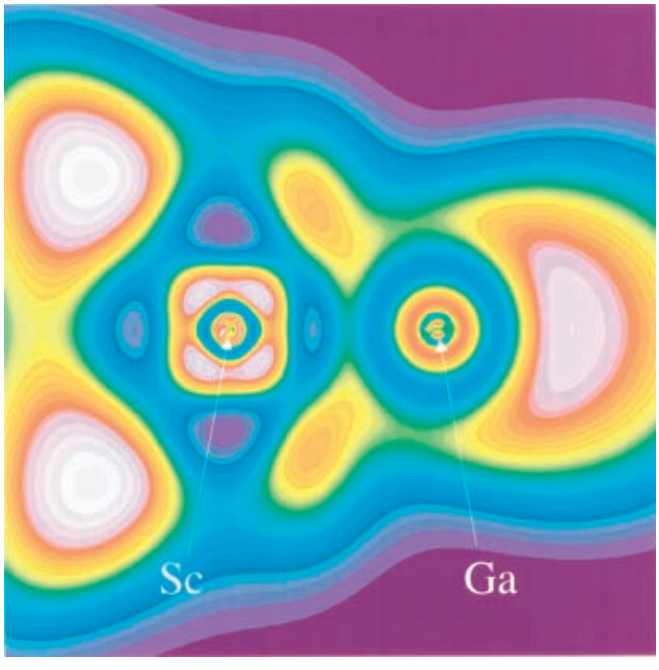

Fig. 5. ELF for the ScGa molecule

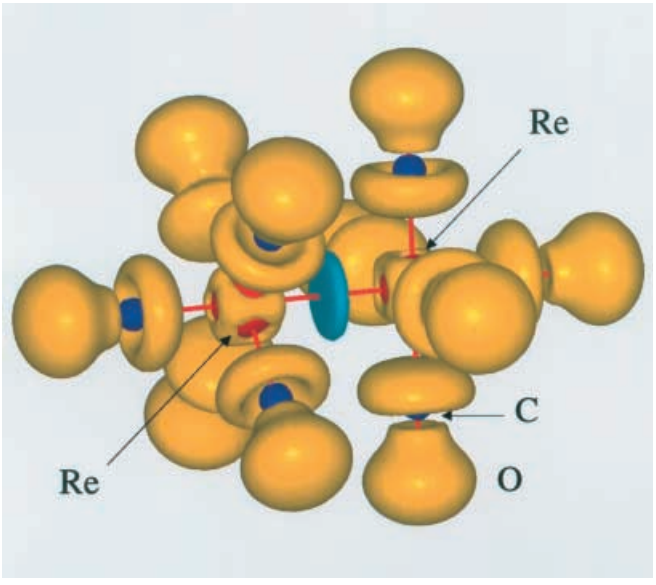

Fig. 6. ELF for the $Re_2(CO)_{10}$ molecule. The *blue* 0.33-localization domain encloses the ELF maximum of the Re–Re bond (η = 0.46) in the valence region. The *brown* 0.66-localization domain illustrates the structuring of the outer-core region of the Re atoms: there are only ELF saddle points on the Re–Re bond line, the ELF maxima point between the ligands

(assuming the *z*-axis is through the metal atoms) [25]. Figure 6 (ADF calculation; bond distances: *d*(Re–Re) = 322.4 pm, *d*(Re–C) = 212 pm, *d*(C–O) = 117.1 pm; dihedral angle 45°) shows the structuring of the ELF outer-core regions of the Re atoms (the brown colored 0.66-localization domains) with an ELF saddle point on the Re–Re connecting line (one in each outer-core region). The ELF maximum in the valence region for the Re–Re bond has the value $\eta = 0.46$ (enclosed by the blue 0.33-localization domain). This relatively low ELF value does not originate from the participation of *d* orbitals, as supposed for the Co–Ti bond in a Ti–Co complex [26]. As already described, the lowering of the ELF values can be achieved only for a uniform occupation of the *d* orbitals. Neither can the low ELF value indicate a highly polar covalent metal–metal bond [26] (bear in mind that even if the electron density shifts from the metal atoms to the ligands, the ELF does not mirror the electron density). Instead, we suggest that the low ELF values between the Re atoms originate from the influence of the two relatively close Re core regions, comparable to the formation of an ELF ring attractor in a copper dimer. (The relatively high ELF values of $\eta \sim 0.8$ for the ELF maxima of the Re–Re and Mo–Mo bonds as found in Ref. [27] are due to the extended Hückel method used in the calculations). The integration of the electron density within the ELF basin sets indicates that in the core basin sets of each Re atom about half of an electron is "missing" (i.e. total of about one electron), which is found in the disynaptic ELF basin of the Re–Re bond. The result confirms the previously described ELF scheme of the interaction of the inner-shell and valence electrons.

The information gained about the specific behavior of the ELF in situations with definite participation of the

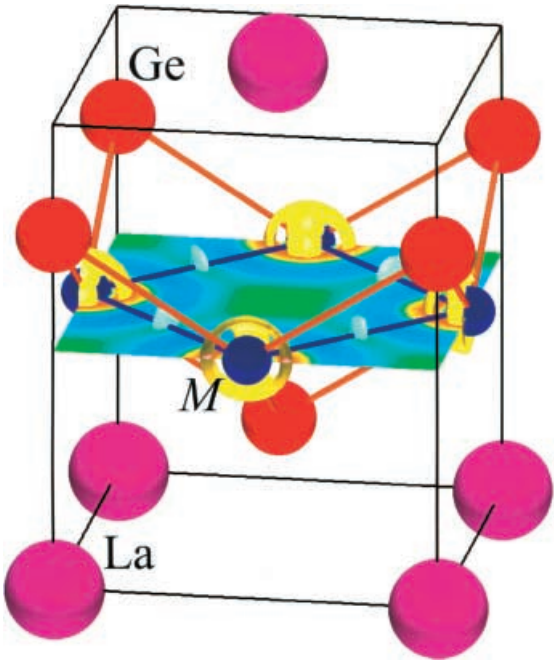

Fig. 7. The structure of LaM_2Ge_2 showing half of the crystallographic unit cell along the *c* direction; the complete unit cell is given by applying the mirror plane located at $z = 1/2\ c$; the *yellow* 0.77-localization domains show the characteristic structuring of the outer-core regions for M = Mn, Fe, Co; the *light-blue* 0.387-localization domains enclose the ELF maxima for the *M*–*M* bond

penultimate shell in chemical bonding also allows new insights into bonding situations for intermetallic compounds with transition metals to be gained. The isostructural compounds LaM_2Ge_2 (M = Mn, Fe, Co, Ni, Cu) crystallize in the $ThCr_2Si_2$ type of structure family; a graphical representation of the structure is given in Fig. 7. Some other members were already subjected to a theoretical bonding analysis [28]. From our investigations in the framework of the ELF we can derive now for one branch of this family the – yet undescribed – occurrence of directed bonding interactions between transition-metal ions forming a planar, net of condensed four-membered rings with similar *M*–*M* distances $d(M–M)$ = 290 – 299 pm. The ELF distribution for M = Mn, Fe and Co with $d(M–M)$ = 297, 291 and 290 pm, respectively, exhibits in the valence region local maxima between the transition-metal atoms (Fig. 8). They are accompanied by a significant and similar structuring of the outer-core region: similar to the molecule $Re_2(CO)_{10}$ only a saddle point in the ELF occurs along the *M*–*M* line and the ELF maxima are found pointing in the direction of the mesh's voids. The findings are compatible with a direct interaction between the transition-metal atoms in these compounds. Among the phases mentioned only the Mn compound reveals unpaired electrons with complex spin ordering [29]. There is no qualitative difference in the valence region between the respective closed- and open-shell calculation; however, there is a structuring of the outer-core ELF region, which has a dependence on the spin model used. This

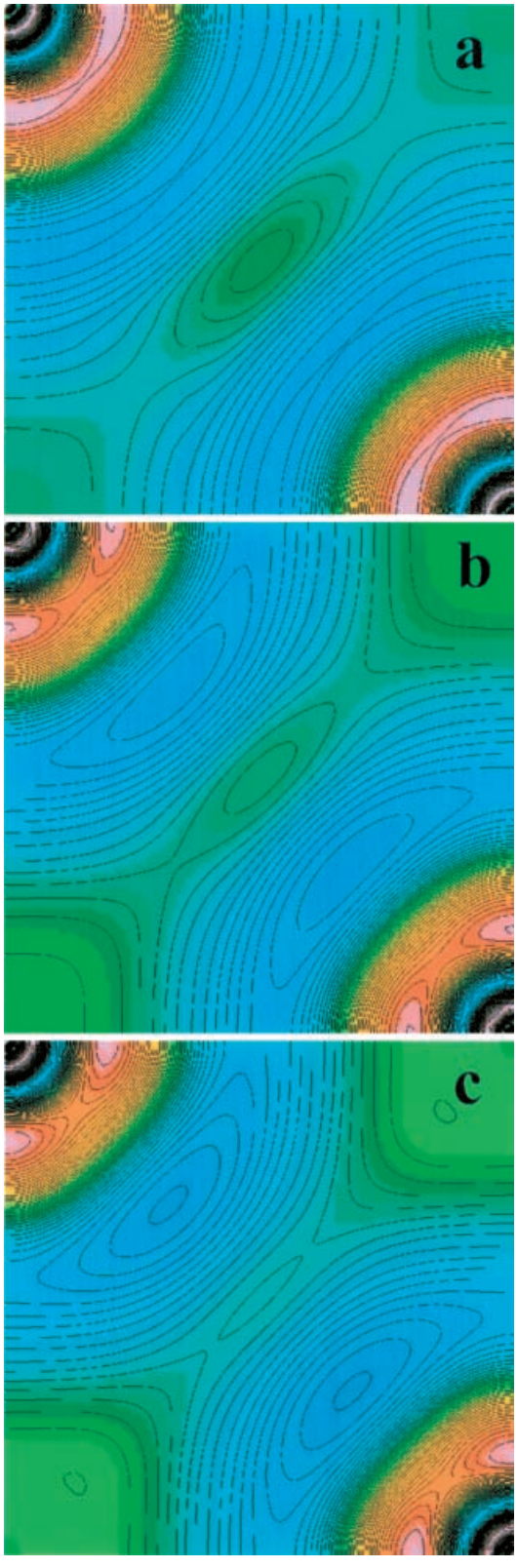

Fig. 8a–c. ELF slices through the planar nets of the transition metals *M*. **a** $LaMn_2Ge_2$ (closed-shell calculation); **b** $LaFe_2Ge_2$; **c** $LaCo_2Ge_2$. An ELF maximum is found in the *M*–*M* midpoint. The outer-core region ELF maxima in the slices presented point between the four bond partners

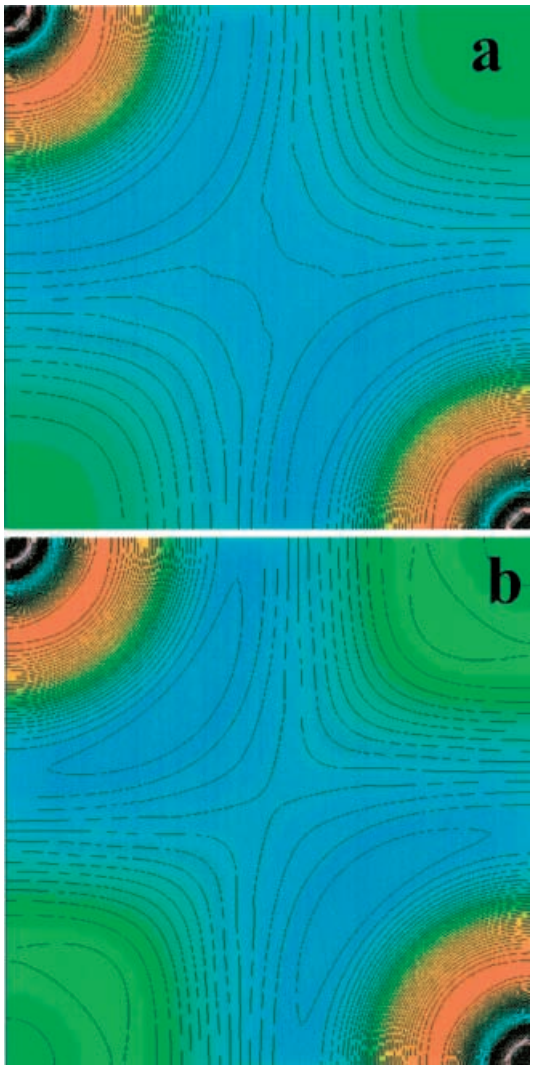

Fig. 9a, b. ELF slices through the planar nets of the transition metals M. **a** $LaNi_2Ge_2$; **b** $LaCu_2Ge_2$. There is no ELF maximum in the valence region and the ELF outer-core region is evidently less structured

dependence will be examined in more detail in the future. In contrast, for M = Ni and Cu, with $d(M–M)$ = 296 and 298 pm, respectively, neither an ELF attractor in the valence region nor a significant structuring of the outer-core region can be observed (Fig. 9), which rules out significant directed interactions between nearest-neighbor metal atoms mediated by d electrons.

5 Conclusions

The participation of transition-metal d electrons in chemical bonding in an ELF representation is accompanied by a significant structuring of the ELF in the outer-core regions, the occurrence of an ELF attractor in the valence region even in the absence of valence-shell electrons and a significant charge excess in the valence region. The inclusion of the outer-core region into the analysis of the ELF reveals valuable information about the participation of the inner-shell electrons in chemical bonding.

Acknowledgements. The authors would like to thank R. Kniep for valuable and exciting discussions. The support of Fonds der Chemischen Industrie is acknowledged.

References

1. Savin A, Nesper R, Wengert S, Fässler TF (1997) Angew Chem Int Ed Engl 36: 1808
2. Becke AD, Edgecombe KE (1990) J Chem Phys 92: 5397
3. Savin A, Jepsen O, Flad J, Andersen OK, Preuss H, von Schnering HG (1992) Angew Chem 104: 186
4. Kohout M, Savin A (1997) J Comput Chem 18: 1431
5. Sun Q, Wang Q, Yu JZ, Kumar V, Kawazoe Y (2001) Phys Rev B 63: 193408
6. Hector LG Jr, Opalka SM, Nitowski GA, Wieserman L, Siegel DJ, Yu H, Adams JB (2001) Surf Sci 494: 1
7. Llusar R, Beltrn A, Andrés, Fuster F, Silvi B (2001) J Phys Chem A 105: 9460
8. Kohout M, Savin A (1996) Int J Quantum Chem 60: 875
9. Silvi B, Savin A, Wagner FR (1997) In: Silvi B, D'Arco P (eds) Modelling of minerals and silicated materials. Kluwer, Netherlands, pp 179–199
10. Bader RFW (1990) Atoms in molecules: a quantum theory. Oxford University Press, Oxford
11. Silvi B, Savin A (1994) Nature 371: 683
12. Savin A, Silvi B, Colonna F (1996) Can J Chem 74: 1088
13. (a) ADF (density functional program ADF2000.01); (b) Baerends EJ, Ellis DE, Ros P (1973) Chem Phys 2: 41; (c) Versluis L, Ziegler T (1988) J Chem Phys 88: 322; (d) te Velde G, Baerends EJ (1992) J Comput Phys 99: 84; (e) Fonseca Guerre C, Snijders JG, G. Velde G, Baerends EJ (1998) Theor Chem Acc 99: 391
14. Vosko SH, Wilk L, Nusiar M (1980) Can J Phys 58: 1200
15. Becke AD (1988) Phys Rev A 38: 3098
16. Lee C, Yang W, Parr RG (1988) Phys Rev B 37: 785
17. Kohout M (2001) DGrid, version 2.3. Max-Planck-Institut für Chemische Physik fester Stoffe, Dresden
18. Jepsen O, Andersen OK (2000) The Stuttgart TB-LMTO-ASA program, version 4.7. Max-Planck-Institut für Festkörperforschung, Stuttgart
19. Kohout M (2001) Basin, version 2.3. Max-Planck-Institut für Chemische Physik fester Stoffe, Dresden
20. Wagner FR (2001) TopAn program system. Max-Planck-Institut für Chemische Physik fester Stoffe, Dresden
21. Hochrein O, Grin Yu, Kniep R (1998) Angew Chem 110: 1667
22. Kohout M, Wagner FR, Grin Y (2001) Max-Planck-Gesellschaft, Jahrbuch 2001. Vandenhoeck and Ruprecht, Göttingen, pp 617–619
23. Joubert L, Silvi B, Picard G (2000) Theor Chem Acc 104: 109
24. Bytheway I, Gillespie RJ, Tang T-H, Bader RFW (1995) Inorg Chem 34: 2407
25. Shriver DF, Atkins PW, Langford CH (1998) Inorganic chemistry, 2nd edn. Oxford University Press, Oxford
26. Jansen G, Schubart M, Findeis B, Gade LH, Scowen IJ, McPartlin M (1998) J Am Chem Soc 120: 7239
27. Fässler TF, Savin A (1997) Chem Unserer Zeit 31: 110
28. (a) Hoffmann R, Zheng C (1985) J Phys Chem 89: 4175; (b) Zheng C, Hoffmann R (1988) J Solid State Chem 72: 58; (c) Zheng C (1993) J Am Chem Soc 115: 1047; (d) Johrendt D, Felser C, Jepsen O, Andersen OK, Mewis A, Rouxel J (1997) J Solid State Chem 130: 254; (e) Gustenau E, Herzig P, Neckel A (1997) J Solid State Chem 129: 147; (f) Gavoille G, Hansen NK, Welter R, Malaman B, Herzig P, Krane H-G (2000) J Phys Condens Matter 12: 2667
29. Welter R, Ijjaali I, Venturini G, Ressouche E, Malaman B (1998) J Magn Magn Mater 187: 278